J. Biochem. **143,** 9–19 (2008)
doi:10.1093/jb/mvm192

Construction and Characterization of Single-chain Antibodies Against Human Insulin-like Growth Factor-I Receptor from Hybridomas Producing 1H7 or 3B7 Monoclonal Antibody

Yu Kusada[1,2], Toru Morizono[1], Ayano Matsumoto-Takasaki[2,3], Keiko Sakai[2,3], Shuma Sato[1,2], Hideki Asanuma[1,2], Atsushi Takayanagi[2,4] and Yoko Fujita-Yamaguchi[1,2,3,*]

[1]Department of Applied Biochemistry, Tokai University School of Engineering, Kanagawa 259-1292; [2]Core Research for Evolutional Science and Technology (CREST), Japan Science and Technology Agency (JST); [3]Institute of Glycotechnology, Tokai University, Kanagawa 259-1292; and [4]Department of Molecular Biology, Keio University School of Medicine, Tokyo 160-8582, Japan

Received September 18, 2007; accepted September 19, 2007; published online October 23, 2007

Recombinant antibody consisting of the single-chain variable fragment (scFv) of 1H7 monoclonal antibody against insulin-like growth factor-I receptor (IGF-IR) and human IgG_1 Fc domain, scFv-Fc, has been found to exhibit inhibitory effects on breast cancer growth *in vitro* and *in vivo* [Li *et al.* (2000) *Cancer Immunol. Immunother.* 49, 243; Sachdev *et al.* (2003) *Cancer Res.* 63, 627]. Various types of scFvs from hybridomas producing 1H7 or 3B7 mAb were constructed using conventional phage display technology to further characterize the specificity and affinity of anti-IGF-IR mAbs. Binding studies performed using either phage antibodies or soluble scFv proteins to IGF-IR or insulin receptor (IR) and IGF-IR pre-incubated with mAbs suggested that (i) 1H7 and 3B7 bind to IGF-IR but do not bind to its structurally related IR, (ii) either the VL–VH or VH–VL sequence order does not apparently affect specificity for IGF-IR and (iii) 1H7 and 3B7 bind the independent epitopes, located in or near the N-terminal (440–514) and C-terminal (62–184) domains of the α subunit, respectively. This study not only revealed new information on binding regions for two anti-IGF-IR mAbs, but also provided the scFv genes as tools for further manipulation of the affinity or development of new IGF-IR-targeted cancer therapeutics.

Key words: epitope specificity, insulin-like growth factor I receptor, insulin receptor, phage display, single-chain antibody.

Abbreviations: Ab, antibody; ABTS, 2,2′-azino-bis (3-ethylbenzthiazoline-6-sulfonic acid); BSA, bovine serum albumin; CBB, Coomassie brilliant blue; CDR, complementarity determining region; cfu, colony formation unit; CH1, constant domain 1 of antibody heavy chain; Con A, concanavalin A; ELISA, enzyme-linked immunosorbent assay; FN, fibronectin; FR, framework region; Fv, variable fragment; GR, glutathione reductase; HRP, horseradish peroxidase; IGF-IR, insulin-like growth factor I receptor; IPTG, isopropyl-β-D-thiogalactopyranoside; IR, insulin receptor; mAb, monoclonal Ab; OVA, ovalbumin; PCR, polymerase chain reaction; PVDF, polyvinylidene difluoride; rhIGFIR, recombinant extracellular domain of human IGF-IR; rhIR, recombinant extracellular domain of human IR; RNase A, ribonuclease A; RT-PCR, reverse transcription PCR; scFv, single-chain variable fragment; SPR, surface plasmon resonance; TBS, Tris-buffered saline; VH, variable region of antibody heavy chain; VL, variable region of antibody light chain.

Since molecular cloning first revealed a complete human insulin-like growth factor-I receptor (IGF-IR) primary sequence two decades ago (*1*), significant advancements have been made towards understanding the role of IGF-IR in cell biology as well as in cancer biology (*2–5*). IGF-I and -II bind to IGF-IR with high affinity, thereby activating IGF-IR tyrosine-kinase, which in turn stimulates downstream signalling cascades. IGF-IR signalling is known to play an important role in proliferation, anti-apoptosis and differentiation. Increased IGF-IR signalling has also been found to contribute to cancer cell growth and progression. In the last decade, numerous studies have focused on testing whether reduction of IGF-IR signalling can inhibit cancer cell growth *in vitro* and *in vivo* (*6*). Examples for such strategies include anti-sense RNA (*7*), tyrosine kinase inhibitors (*8*) and IGF-IR-extracellular domain-specific antibodies (*9–13*).

In order to develop cancer therapeutics, the authors previously constructed a single-chain variable fragment (scFv) from the variable domains of 1H7 monoclonal antibody (mAb) (*14*), produced it as a chimeric form, scFv-Fc, consisting of anti-IGF-IR mouse scFv and human IgG1 Fc domain, and demonstrated its inhibitory effects on MCF-7 tumour growth (*9*). The inhibitory effects of the scFv-Fc on breast cancer cell growth *in vitro* and *in vivo* were later found to be caused by down-regulation of IGF-IR in MCF-7 and T61 tumours

*To whom correspondence should be addressed. Tel: +81-463-58-1211 (ex. 4188), Fax: +81-463-50-2012,
E-mail: yamaguch@keyaki.cc.u-tokai.ac.jp

(*13*, *15*). Since then, down-regulation followed by degradation has been implicated as a major mechanism for several other anti-IGF-IR antibodies that exhibit inhibitory effects on cancer growth as well (*10–12*). More recently, 24 h pre-treatment with anti-IGF-IR antibodies was shown to inhibit insulin-mediated phosphorylation of insulin receptor (IR) and insulin-stimulated proliferation of MCF-7 cells presumably *via* lipid rafts where IR appears to exist in close physical proximity to IGF-IR (*16*). This intriguing observation may provide an additional rationale for development of anti-IGF-IR antibody-based cancer therapy since several pieces of evidence suggest that an exon 11-lacking IR isoform A is predominantly expressed in malignant cells and acts as a growth factor receptor (*17*, *18*).

In the current study, various types of scFvs were constructed using conventional phage display technology from hybridomas producing 1H7 or 3B7 mAb in order to further characterize the specificity and affinity of anti-IGF-IR mAbs (*14*, *19*). Binding assays were performed utilizing either phage antibodies or soluble scFv proteins, which demonstrated that 1H7 and 3B7 bind to IGF-IR but do not bind to its structurally related IR and that either the VL–VH or VH–VL sequence order does not apparently affect specificity for IGF-IR. Moreover, competition binding studies with a combination of mAbs revealed that 1H7 and 3B7 bind to the independent epitopes and that the regions to which 1H7 and 3B7 bind correspond to epitopes previously proposed for mAbs 24–57 and 16–13, residues 440–514 and 62–184 of the α subunit, respectively (*20*, *21*). This study thus provided valuable information on the specificity for two anti-IGF-IR mAbs and on scFv genes as tools for further manipulation of the affinity or development of new IGF-IR-targeted cancer therapeutics.

MATERIALS AND METHODS

Materials—Recombinant human extracellular domain of IGF-IR (rhIGF-IR) and IR (rhIR) were purchased from R&D Systems Inc. (MN, USA). Concanavalin A (Con A), ribonuclease A (RNase A) and ovalbumin (OVA) were obtained from Sigma-Aldrich (MO, USA). ABTS/H_2O_2 and glutathione reductase (GR) were from Roche Diagnostics (Mannheim, Germany). Fibronectin (FN) was purified by gelatin-affinity chromatography from bovine sera as previously described (*22*). *Escherichia coli* strains used were the suppressor strain TG1, and the non-suppressor strain TOP10F' from Invitrogen (CA, USA). *Escherichia coli* JM109 was the suppressor strain and was purchased from Takara Bio (Shiga, Japan). Helper phage M13KO7, HRP/anti-M13 conjugate, HRP/anti-E tag conjugate and phagemid vector pCANTAB5E were purchased from GE Healthcare Bio-Sciences Corp. (NJ, USA). Anti-IGF-IR mAbs, 1H7 and 3B7, were either purified from hybridoma culture media by conventional methods or purchased from Santa Cruz (CA, USA). Anti-IGF-IR mAbs, 24–57 and 16–13, were from BioSource International (CA, USA) and Cell Science (MA, USA), respectively. DNA primers used in this study were designed accordingly and ordered from Nihon Gene Research Laboratories Inc. (Sendai, Japan).

Preparation of Anti-Human IGF-IR scFv Genes from Hybridoma-Producing 1H7 or 3B7 mAb—In this study, four types of anti-IGF-IR scFv genes, designated as 1H7, 1H7R, 3B7 and 3B7R, were prepared from hybridoma cells producing 1H7 or 3B7 mAb (*14*, *19*). 1H7 scFv (VL–VH form) was prepared as described previously (*9*). For construction of the modified version of 1H7R (VH–VL form), the original 1H7 scFv gene was used as a template. 1H7 VH and VL genes were amplified by PCR with primers (1H7 VH forward-1: 5′-GGGTTCCGGCCCAGCC GGCCGAAGTAAAAGTGGTGG-3′, 1H7 VH reverse 1: 5′-TGAACCACCGCCGCTACCGCCTCCGCCTGAGGAGA CGGTGACC-3′, 1H7 VL forward 1: 5′-CAGTGGTGGAG GATCTGACATTGTGATGACCCAGT-3′, 1H7 VL reverse 1: 5′-CCTTGTAGCGGCCGCTTTTATTTCCAGATTGG TC-3′). After amplified VH and VL genes were purified, VH gene was further amplified by second PCR to include the linker sequence with the primers (1H7 VH forward 1, 1H7 VH reverse 2: 5′-AGATCCTCCACCACTGCCGCC ACCTCCTGAACCACCGCCGCT-3′). The resulting VH and VL genes were joined by assembly PCR under the following conditions: pre-heating at 94°C for 1 min, and 10 cycles of denaturing at 94°C for 1 min, annealing at 52°C for 1 min and extension at 68°C for 1 min. The linked VH–VL gene was further amplified by PCR with primers (1H7 VH forward 1, 1H7 VL reverse 1) under the following conditions: pre-heating at 94°C for 1 min, and 35 cycles of denaturing at 94°C for 1 min, annealing at 61°C for 1 min and extension at 72°C for 1 min. For construction of the 3B7 scFv gene, RNA was extracted from 3B7-secreting hybridoma cells (5×10^6) with a Trizol reagent (Invitrogen). Total RNA (2 μg) was reverse-transcribed with ImPromIIreverse transcriptase (Promega) according to the manufacturer's protocol. With the resulting cDNA (500 ng) as a template, 3B7 VH and VL genes were amplified by PCR using various combinations of the primer sets according to a previously described method with some modifications (*23*). After pre-heating at 94°C for 5 min, PCR was carried out with 40 cycles under conditions of denaturing at 94°C for 30 s, annealing at 55°C for 1 min and extension at 68°C for 1 min. The amplified VH and VL genes were purified by 1% agarose gel electrophoresis and subjected to assembly PCR. VH and VL genes, 250 ng each, were mixed and assembly PCR was carried out with 10 cycles under conditions of denaturing at 94°C for 10 s, annealing at 55°C for 30 s and extension at 68°C for 1 min followed by second PCR amplification using the primer set (3B7 forward 1: 5′-GAGGAGGAGGCGGGGCCCAGCCGGCC GA-3′, 3B7 reverse 1: 5′-GAGGAGGAGGCGGCCGCATA GTGACA-3′) with 30 cycles under conditions of denaturing at 94°C for 15 s, annealing at 55°C for 1 min and extension at 68°C for 90 s. The resulting scFv gene was purified by agarose gel electrophoresis. Although the constructed 3B7 scFv-presenting phage showed high affinity, its corresponding 3B7 scFv protein was never produced (unpublished data). Since the constructed 3B7 scFv gene was found to contain a portion of the CH1 region due to the primers used, testing was performed to find out whether the removal of the CH1 peptide improves the production of scFv protein. Therefore, a new version of the 3B7 scFv gene was prepared by PCR

to exclude the CH1 portion with the primer set of 3B7 forward 2: 5′-TTGTTCCTTTCTATGCGGCCCAGCCGGC CGAGCTCG-3′ and 3B7 reverse 2: 5′-CCTTGTAGCG GCCGCTGAGGAGACTGTGAGAGTGGTGCCTTGG-3′. PCR was carried out under conditions of pre-heating at 94°C for 1 min, and 30 cycles of denaturing at 94°C for 20 s, and annealing/extension at 68°C for 1 min. Similarly, a 3B7 scFv modified version, 3B7R (VH–VL form), was also constructed. VH gene was amplified with the primer sets (3B7 forward 3: 5′-GGGTTCCGGCCCAGCCGGCCCTCG AGGTGAAGCTGGTGGAGTCTGGAC-3′, 3B7 reverse 3: 5′-GCCACCGCCACCAGAGGATGAGGAGACTGTGAGA GTGGTGC-3′) followed by second amplification to include the linker sequence with the primer sets (3B7 forward 3 and 3B7 reverse 4: 5′-ACCACCCCCACCACCGCCCGAGC CACCGCCACCAGAGGATGAGG-3′). VL gene was amplified with the primer set (3B7 forward 4: 5′-CTCTAGA TCTTCCGAGCTCGATGCTGTTGTGACTCAGGAATCT GC-3′, 3B7 reverse 5: 5′-CCTTGTAGCGGCCGCGCCTAG GACAGTCAGTTTGGTTCCTCCACCG-3′) followed by second amplification to include the linker sequence with the primer set (3B7 forward 5: 5′-GGGCGGTGGTGGGG GTGGTTCCTCTAGATCTTCCGAGCTCGATGCTG-3′, 3B7 reverse 5). The resulting VH and VL genes were joined by assembly PCR under the following conditions: pre-heating at 94°C for 1 min followed by 10 cycles of denaturing at 94°C for 20 s, annealing at 63°C 30 s and extension at 72°C for 40 s. The assembled gene was further amplified using the primer set (3B7 forward 3, 3B7 reverse 5) under the conditions of pre-heating at 94°C for 1 min and 30 cycles of 94°C for 1 min, and annealing/extension at 68°C for 1 min. The final scFv gene product was gel-purified.

Preparation of Four Types of scFvs-Displaying Phages—Construction of phage displaying scFvs was performed according to instructions for the 'Expression Module/Recombinant Phage Antibody System' supplied by GE Healthcare with some modifications as described (*24*). All scFv genes prepared were digested with restriction enzymes *Sfi* I and *Not* I. Digested scFv genes were purified and ligated with pCANTAB5E vector by incubation with Ligation High (TOYOBO) for 1 h. The ligated vectors, precipitated by ethanol and dissolved in ultra-pure water, were transformed to *E. coli* JM109 strain and cultured on LB (1% tryptone, 0.5% yeast extract, 1% NaCl and 1 mM NaOH) supplemented with 2% glucose and 50 μg/ml carbenicillin (LBGC) plates. After confirmation of the insert by colony PCR, each colony was cultured in 40 ml of SBSC at 25°C for 2 h followed by infection with 8.8×10^{10} pfu M13KO7 helper phage for 1 h at 37°C. Infected *E. coli* was selected by culturing in the presence of 50 μg/ml kanamycin at 25°C for 2 d. The culture supernatants containing phages were precipitated in 4% polyethylene glycol/0.5 M NaCl (PEG precipitation) and resuspended in TBS (20 mM Tris–HCl buffer, pH 7.4, containing 0.15 M NaCl) containing 1.5% BSA and 0.2% Tween 20 followed by treatment with benzonaze (Novagen) to digest any unnecessary DNA. The titre (cfu) of each phage was determined by means of infection activity against *E. coli* TG1 cells. Each resulting phage was subjected to ELISA.

Expression of Four Types of scFv Proteins—Escherichia coli TOP10F', non-suppressor strain, harbouring a chaperon/repressor vector carrying a spectinomycin resistance gene, that was produced by Takayanagi *et al*. (manuscript in preparation) was infected with phages, followed by selection on LBGC agar plates in the presence of 50 μg/ml of spectinomycin (LBGCS). Once colonies were confirmed to have the scFv gene by colony PCR, *E. coli* cells were cultured overnight in 5 ml of 2 × YT medium containing 50 μg/ml carbenicillin, 50 μg/ml spectinomycin (2 × YTCS) and 1% glucose at 25°C. Overnight culture solution was re-cultured in 40 ml of freshly-prepared 2 × YTCS for 1 h at 30°C, followed by induction with 1 mM IPTG at 30°C for 5 h. Periplasm fractions, which were prepared by means of mild osmotic shock, were used for SDS–PAGE/western blotting analysis, ELISA and purification.

Purification of 1H7 or 3B7R scFv Protein—The expressed scFv proteins were purified using anti-E tag Ab/Protein-G gel column that was prepared by conjugating anti-E tag antibody (GE Healthcare Bio-Sciences) covalently to Seize X Protein G gel column (Pierce) according to the manufacture's protocol. *Escherichia coli* periplasm extracts were prepared as described earlier and filtered, to which 10 × TBS was added. The column was incubated with the periplasm extract at RT for 1 h. After the column was washed with TBS, bound 1H7 or 3B7R scFv protein was eluted with 0.1 M glycine-HCl, pH 2.8. Eluates were immediately neutralized with 1 M Tris–HCl, pH 9.5. The 1H7 scFv protein was further purified by gel filtration using a Superdex 200 column ($10 \times 300\,mm^2$; GE Healthcare Bio-Sciences) equilibrated with 10 mM HEPES, pH 7.4, containing 150 mM NaCl and 0.05% Tween-20 (the running buffer for SPR analyses) at a flow rate of 0.4 ml/min. Elution was monitored by absorbance at 280 nm. Fractions (0.5 ml each) containing monomer forms of 1H7 scFv were used for SPR analyses.

Evaluation of Specificity by ELISA—Binding of phage antibodies or soluble scFv proteins to IGF-IR was evaluated by ELISA. Each well of a 96-well plate was coated with 500 ng/50 μl of rhIGF-IR or rhIR followed by incubation for 2 h at RT. Antigen-coated wells and control wells were blocked by incubation overnight with 150 μl of 3%BSA/TBS at 4°C. The wells were then incubated with 50 μl of phage antibodies or soluble scFv proteins at RT for 2 h. The wells were washed 3 times with 150 μl of TBS containing 0.2% Tween-20 (TBST). For detection of phage antibodies, HRP/anti-M13 conjugate (1:2,500 dilution) was used as a second antibody. For detection of scFv proteins, HRP/anti-E-tag conjugate (1:2,000 dilution) was used as a second antibody. The wells were washed seven times with TBST and then three times with TBS. Peroxidase activity was detected by reaction with 100 μl of ABTS/H_2O_2 for 30 min and termination with 1% oxalic acid. The absorbance at 415 nm was measured by a BIO-RAD plate-reader. In addition to BSA, which was always used as a control for ELISA, other proteins including FN, GR, Con A, RNase A and OVA were examined as antigens (coated to wells at 500 ng/50 μl) for their reactivity to the 1H7 or 3B7 scFv.

Competition Assays—ELISA-based competition assays were performed to confirm that constructed phages presenting scFvs retain the same epitope specificity as their parental 1H7 or 3B7 mAb and to analyze their epitope specificity. Antigen-coated wells were prepared

and blocked by BSA as described earlier, followed by pre-incubation of the wells with 1H7 or 3B7 mAb, respectively, in order to block their respective epitopes. Phage antibodies were then added to the wells coated with either 1H7 mAb-bound or 3B7 mAb-bound IGF-IR. After incubating RT for 2 h, phage antibodies were detected with HRP/anti-M13 conjugate as a second antibody. Washing procedures and the detection of HRP activity were performed as above. Similar competition binding assays were carried out for 1H7 or 3B7R scFv to the IGF-IR pre-incubated with 100 nM of mAbs including 24–57 and 16–13.

ELISA-based measurements of dissociation constant (K_D) were performed as described previously (*25*, *26*). Briefly, antibodies were incubated with excess concentrations of antigens at 4°C overnight. Equilibrated antibodies/antigens complexes were transferred to wells coated with antigens that were blocked with BSA. After incubation at RT for 1 h, the wells were washed and bound antibodies were detected by adding secondary antibodies as described above. K_D was determined as previously described (*25*, *26*).

Characterization of Phage Antibodies, mAbs and Purified scFv Proteins by Surface Plasmon Resonance (SPR)—SPR analysis was carried out at 25°C using 10 mM HEPES, pH 7.4, containing 150 mM NaCl and 0.005% surfactant P20 (HBS-P buffer) as a running buffer. Binding properties of phage antibodies were determined using a Biacore X (Biacore Inc., Uppsala, Sweden). A CM3 sensor chip was equilibrated overnight with the running buffer before use. Immobilization of the antigen on the sensor chip was achieved by injecting 50 µl of 10 mM sodium acetate buffer, pH 5, containing 500 µg/ml of rhIGF-IR *via* amine groups using the Amine Coupling Kit (Biacore Inc.). Binding of phage antibodies displaying 1H7 scFv was analysed at three different concentrations as indicated in the figure legend. M13KO7 helper phage that does not display scFv, was used as a negative control whereas 1H7 mAb was used as a positive control.

SPR analyses of the purified 1H7 mAb, 1H7 scFv protein, 3B7 mAb as well as 3B7R scFv protein to rhIGF-IR were performed at 25°C on a Biacore3000 biosensor (Biacore Inc.). RhIGF-IR was immobilized on the CM5 sensor chip using the amine coupling kit supplied by the manufacture. Binding of scFv to rhIGF-IR on the surface of the sensor chip was monitored at a flow rate of 20 µl/min. The rates of association (k_a) and dissociation (k_d) for scFvs and mAbs were determined using BIAevaluation version 3.0 software (Biacore Inc.) by monovalent and divalent models, respectively (*27*). The thermodynamic K_D was calculated by dividing k_d by k_a.

RESULTS

Preparation of Four Types of scFvs-Displaying Phages from Hybridomas Producing 1H7 or 3B7 mAb—First phage antibody, phages displaying anti-IGF-IR scFvs, was constructed from the 1H7 scFv-Fc gene, which was previously isolated and constructed as described (*9*). After positive phages were identified by ELISA, SPR analyses were carried out to determine whether or not

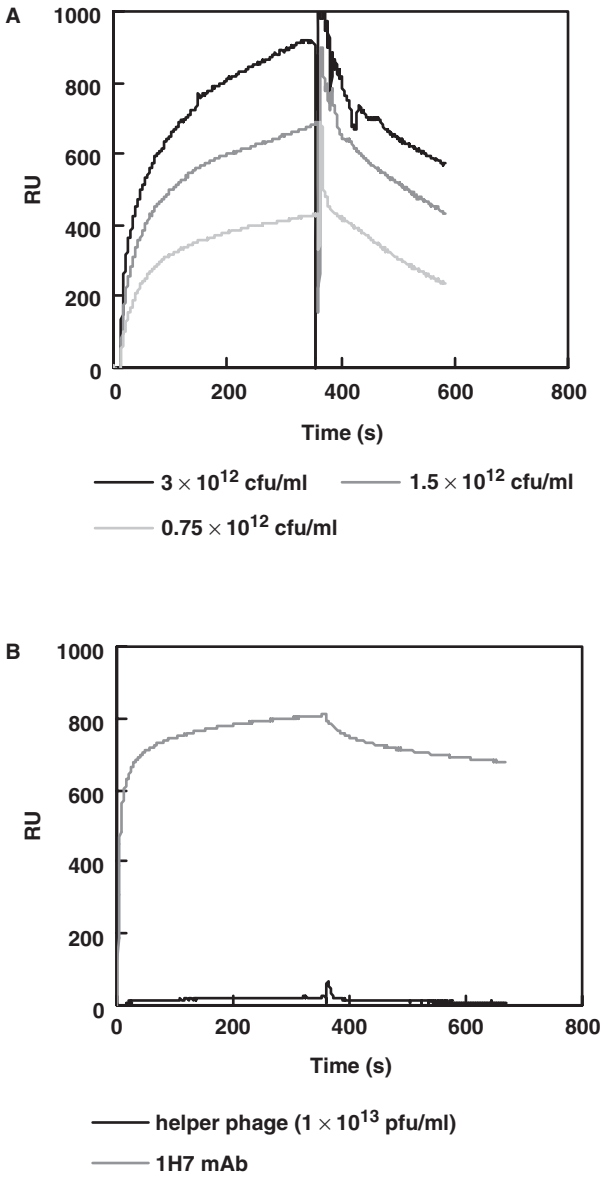

Fig. 1. **SPR analyses of scFv-presenting phage antibodies.** Phage antibodies at indicated concentrations were passed over the rhIGF-IR-immobilized CM3 chip at a flow rate of 5 µl/min as described in the 'MATERIALS AND METHODS' section. (A) Sensorgrams obtained for the phage antibody displaying 1H7 scFv. (B) Sensorgrams for helper phage and 1H7 mAb, which were analysed as a negative and positive control, respectively.

phages displaying 'anti-IGF-IR' scFvs have binding affinities for IGF-IR. Figure 1A shows sensorgrams at different concentrations of phages displaying 1H7 scFvs. Although the data are merely qualitative, the resulting sensorgrams clearly indicated that the phage antibodies bound to immobilized IGF-IR in a dose-dependent manner. In contrast, the helper phage that does not display scFvs did not bind to IGF-IR (Fig. 1B), indicating that the binding kinetics detected by SPR were due to the anti-IGF-IR scFvs displayed by phages and not by the phage by itself. As a positive control, a sensorgram of 1H7 mAb binding to IGF-IR is included in Fig. 1B.

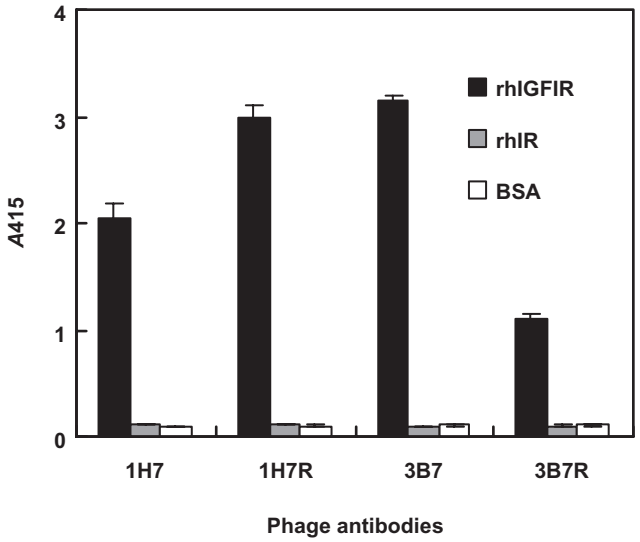

Fig. 2. **Binding specificities of phage antibodies displaying 1H7 (VL–VH), 1H7R (VH–VL), 3B7 (VL–VH) and 3B7R (VH–VL) scFvs as determined by ELISA.** Binding of phage antibodies to rhIGF-IR, rhIR or BSA was examined by ELISA as described in the 'MATERIALS AND METHODS' section. Concentrations of phages used for assays were 1×10^{12} cfu/ml for 1H7 and 1H7R, and 1×10^{10} cfu/ml for 3B7 and 3B7R. The error bars represent the SD calculated from replicates ($n = 3$).

The anti-IGF-IR scFv-Fc construct originally published consisted of the variable domains of 1H7 mAb in a signal peptide-VL-linker-VH order with a C-terminal that was conjugated to human IgG_1 Fc (*9*). 1H7R (VH–VL) was prepared in order to compare potential differences between the original type scFv in a VL–VH order and its reversed VH–VL type scFv. Furthermore, another set of scFv genes was constructed from hybridoma producing 3B7 mAb, which exhibited growth-stimulatory effects (*19*). Thus, four types of scFvs, 1H7 (VL–VH), 1H7R (VH–VL), 3B7 (VL–VH) and 3B7R (VH–VL), were expressed as phage antibodies by conventional phage display techniques. Figure 2 shows the results of ELISA for the four different phage antibodies prepared. The results demonstrated that the order of the variable domains, either VH–VL or VL–VH, does not seem to affect the specificity and affinity of scFvs and that both VH–VL and VL–VH types of 1H7 and 3B7 scFvs are specific for IGF-IR. None of them bound to IR, which shares a high level of sequence homology with IGF-IR (*1*).

Expression and Characterization of Soluble scFv Proteins—To further characterize the binding specificity of four types of scFvs prepared from hybridomas as above, scFv proteins were expressed in *E. coli* Top10F′ harbouring chaperon/repressor vector (Top10F′-Fs) by infection with 1H7, 1H7R, 3B7 or 3B7R phages. After induction with IPTG, the periplasm fractions of *E. coli* Top10F′-Fs transfectants were collected and analysed by SDS–PAGE (Fig. 3A), followed by immunoblotting with anti-E tag antibody to check the expression levels of scFv proteins (Fig. 3B). Binding specificities of IPTG-induced samples were analysed by ELIZA using IGF-IR, IR or BSA as an antigen (Fig. 3C). All four anti-IGF-IR scFvs proteins expressed showed high affinity for IGF-IR but no cross-reactivity with IR (Fig. 3C). This result is in good agreement with the results of ELISA obtained with phage antibodies (Fig. 2). A point of note, however, is that the extent of ELISA signals among different constructs cannot be readily compared at this stage since actual scFv protein concentrations were not normalized.

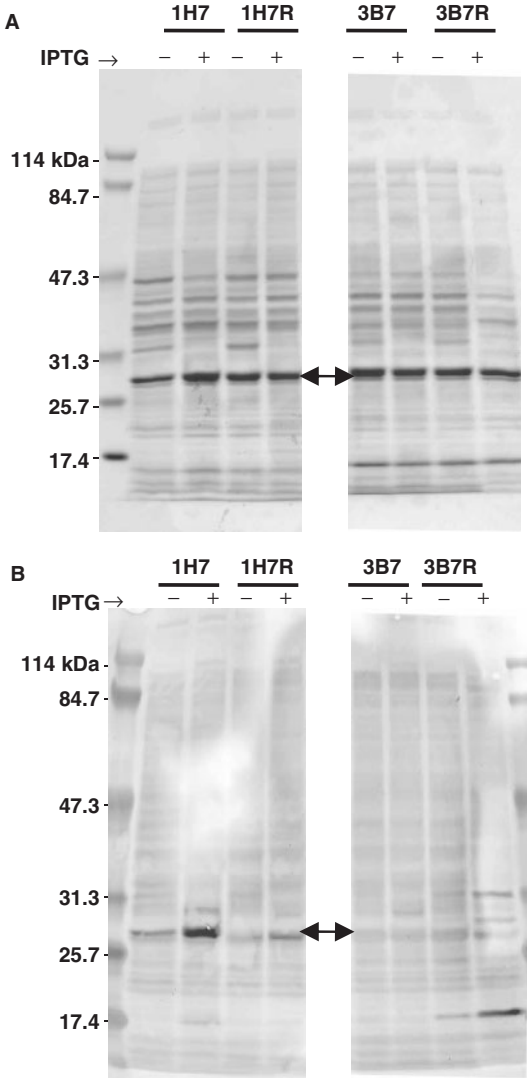

Fig. 3. **Expression and binding specificities of 1H7 and 3B7 scFv proteins.** (A) SDS–PAGE analysis of periplasmic fractions prepared from *E. coli* TOP10F'-Fs infected with 1H7, 1H7R, 3B7 or 3B7R phage. Three micrograms of total protein of each clone, without (–) or after (+) induction with IPTG, were analysed by SDS–PAGE and stained with Coomassie brilliant blue. (B) Western blot analysis of scFv proteins with HRP/anti-E tag antibody (1:2,000 dilution) was performed as described in the 'MATERIALS AND METHODS' section. The arrowheads show the position for expressed scFv proteins. (C) Binding of soluble scFv proteins to rhIGF-IR, rhIR, or BSA was analysed by ELISA in which a 10-fold diluted periplasmic fraction as shown in (A: IPTG +) was used. Bound scFv proteins were detected by HRP/anti-E tag antibody (1:2,000 dilution). The error bars represent the SD calculated from replicates ($n = 3$).

The specificity of 1H7, 1H7R, 3B7 or 3B7R scFv protein was further evaluated by ELISA using non-related proteins as antigens. As seen in Fig. 4, specific binding of 1H7, 3B7 and 3B7R scFv proteins to IGF-IR was confirmed except that their reactivity to GR was noticeable. Compared to those three scFv proteins, 1H7R scFv protein exhibited relatively high reactivity to GR as well as other non-related proteins. A point of note is that although the 1H7R scFv protein showed non-specific binding to some other proteins, it did not bind to the structurally closely related IR or BSA, a commonly used negative control.

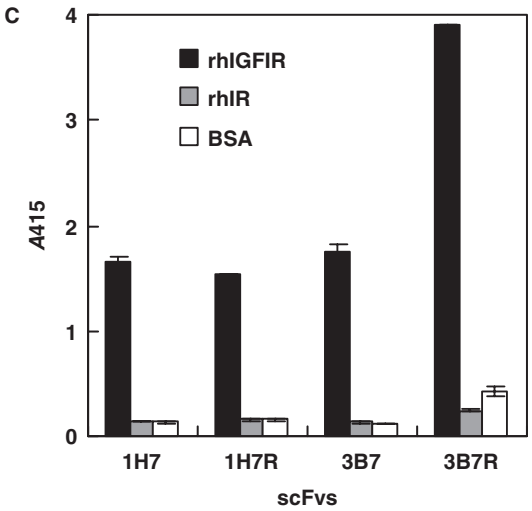

Fig. 3. Continued.

Comparison of the Epitope Recognized by 1H7 or 3B7—The epitope specificities of 1H7 and 3B7 were examined by binding of 1H7 (VL–VH), 1H7R (VH–VL) and 3B7 (VL–VH) phage antibodies to IGF-IR that was pre-incubated with increasing concentrations of either 1H7 mAb or 3B7 mAb (Fig. 5). The binding of both 1H7 and 1H7R phages to IGF-IR was significantly inhibited in the presence of 100 and 1000 nM 1H7 mAb but was not affected by 3B7 mAb (Fig. 5A and B, respectively). Likewise, the binding of 3B7 scFv (VL–VH) phage to IGF-IR was almost completely inhibited in the presence of 100 nM 3B7 mAb but was not affected by 1H7 mAb (Fig. 5C). These results indicated that 1H7 and 3B7 bind to different epitopes on the IGF-IR.

Comparison of the Epitopes Recognized by 1H7 or 3B7 with those of mAbs 24–57 and 16–13—1H7 mAb inhibited IGF-I and -II binding to IGF-IR (*14*) whereas 3B7 mAb stimulated their binding to the receptor (*19*). Soos *et al.* (*20*) characterized a panel of their mAbs against IGF-IR, and demonstrated that mAb 16–13 that stimulated IGF binding and 24–57 that inhibited IGF binding bound to the deduced epitopes of 62–184 and 440–586, respectively. The binding region for 24–57 mAb was later reported to be localized to residues 440–514 (*21*). When 24–57 and 16–13 mAbs were pre-incubated with IGF-IR bound on the plate and the binding of 1H7 and 3B7R scFv proteins to the receptor were then examined, 24–57 and 16–13 mAbs were found to inhibit 1H7 and 3B7R

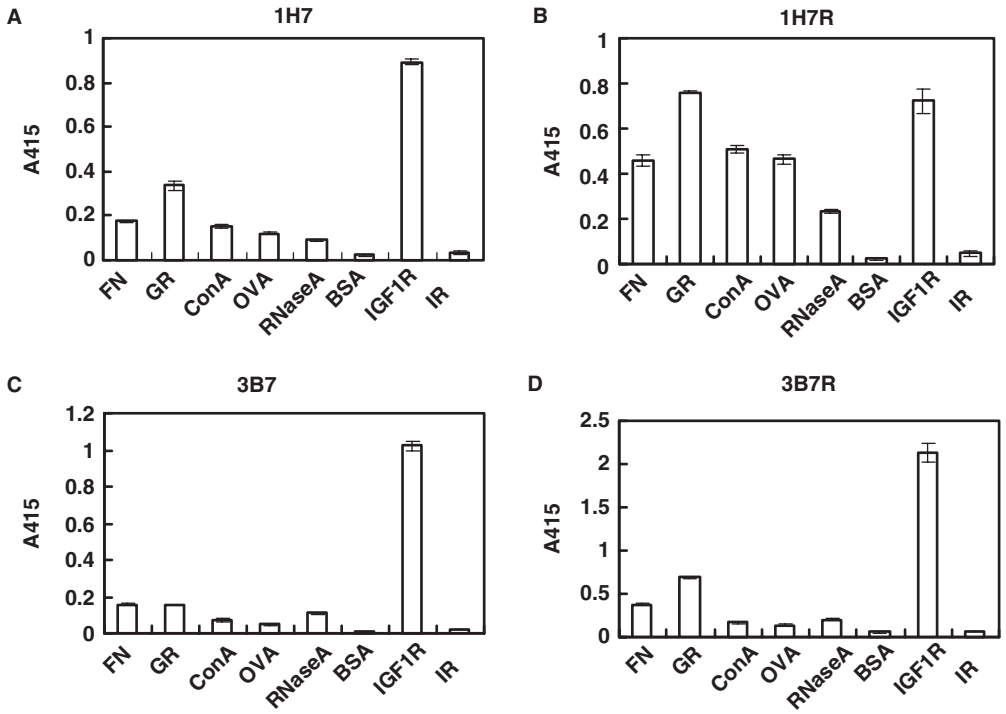

Fig. 4. **Binding of 1H7 and 3B7 scFv proteins to a variety of proteins in addition to IGF-IR, IR and BSA as analyzed by ELISA.** Binding of soluble scFv proteins to proteins as indicated in addition to rhIGF-IR, rhIR and BSA was analysed by ELISA using a 10-fold diluted periplasmic fraction as shown in (Fig. 3: IPTG +). Bound 1H7, 1H7R, 3B7 or 3B7R scFv proteins were detected by HRP/anti-E tag antibody (1:2,000 dilution). The error bars represent the SD calculated from replicates ($n = 3$).

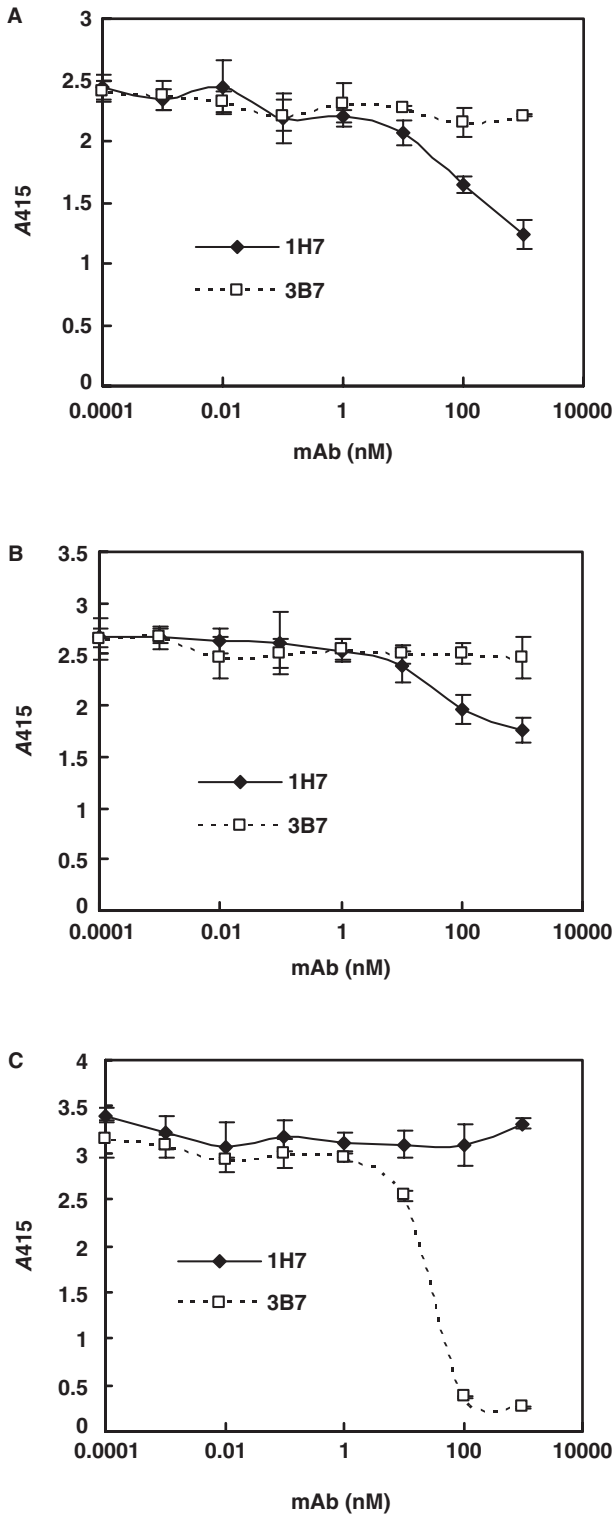

Fig. 5. **Comparison of the epitope recognized by 1H7 or 3B7 by ELISA-based competitive binding studies.** Phage antibody clones displaying scFv, 1H7 at 1×10^{12} cfu/ml (A), 1H7R at 1×10^{12} cfu/ml (B), or 3B7 at 1×10^{10} cfu/ml (C), were added to immobilized rhIGF-IR that had been pre-incubated with parental mAbs [1H7(filled square) or 3B7(open square)] at various concentrations as indicated. The bound phages were detected by HRP/anti-M13 conjugate. The error bars represent the SD calculated from replicates ($n = 3$).

scFv binding to the receptor, respectively (Fig. 6A and B). These results thus strongly indicated that 1H7 and 24–57 mAbs bind to epitopes located in the α subunit (440–514) close to the C-terminus, whereas 3B7 and 16–13 mAbs bind to epitopes located in the N-terminal domain (62–184).

Purification and Characterization of scFv Proteins—The 1H7 and 3B7R scFv proteins that were expressed at a high level (Fig. 3) were purified by anti-E tag Ab affinity chromatography. SDS–PAGE analysis of the eluted protein revealed that 1H7 and 3B7R scFv proteins were purified to near homogeneity (Fig. 7A and B). The purified 1H7 and 3B7R scFv proteins bound to rhIGF-IR in a concentration-dependent manner (Fig. 8A and B).

The 1H7 scFv protein preparation was further purified by gel-filtration to isolate its monomer form, which was subjected to SPR analyses (Fig. 8C). The affinity-purified 3B7R preparation was analysed by SPR (Fig. 8D).

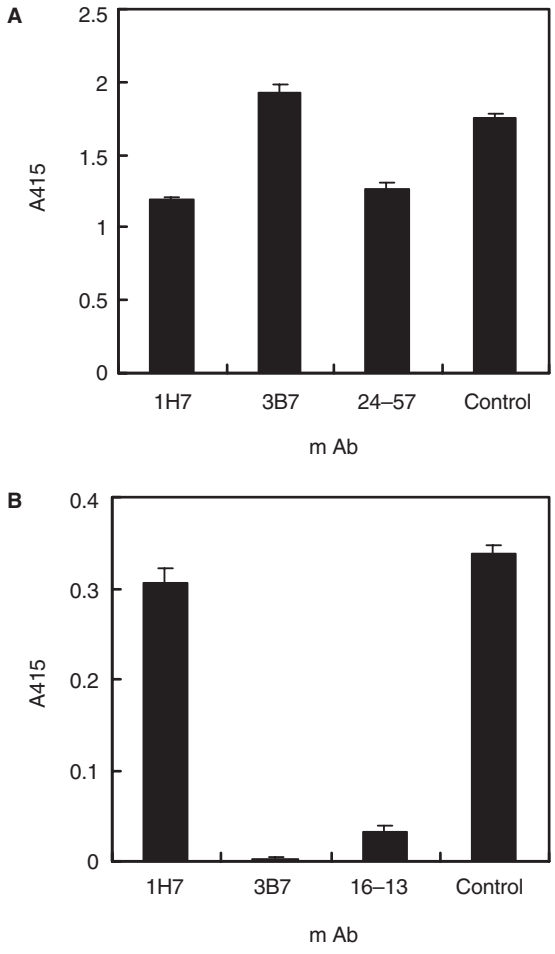

Fig. 6. **Comparison of the epitope recognized by 1H7 or 3B7 mAb with that of 24–57 or 16–13 mAb by ELISA-based competition assays.** Periplasmic fractions containing 1H7 (A) or 3B7R (B) protein were added to immobilized rhIGF-IR that had been pre-incubated with 100 nM of 1H7, 3B7, 24–57 or 16–13 mAb (*21*) as indicated. Bound 1H7 (A) or 3B7R (B) scFv protein was detected by HRP/anti-E tag antibody (1:2,000 dilution). The error bars represent the SD calculated from replicates ($n = 3$).

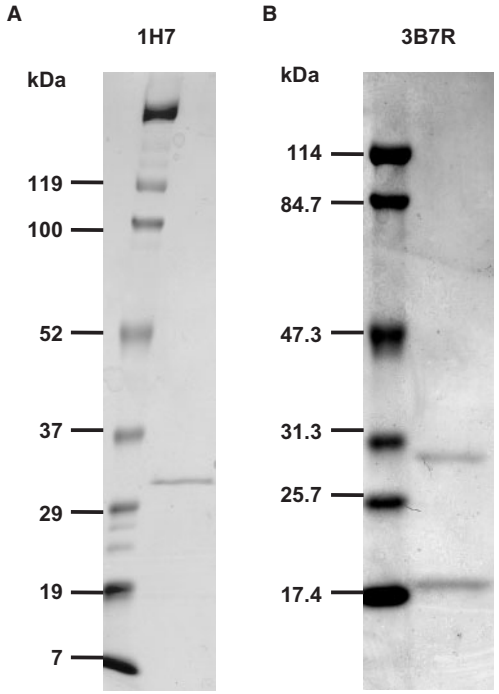

Fig. 7. **SDS–PAGE analysis of purified 1H7 or 3B7R scFv protein.** 1H7 scFv protein (A) or 3B7R (B) scFv protein purified from periplasm of host *E. coli* by E-tag affinity chromatography was analysed together with molecular size markers as indicated by SDS–PAGE and CBB staining.

Affinity constants (K_D) for scFv proteins were calculated based on these analyses. The results are tabulated in Table 1 along with affinity constants of their parental mAbs as well as the results of ELISA-based affinity measurements for 1H7 antibodies. These studies suggested that both 1H7 and 3B7R scFv proteins possess high enough affinity to be successfully used to developing cancer-targeted therapies, and that both 3B7R scFv and its parental 3B7 mAb have higher affinity for IGF-IR than 1H7 counterparts.

DISCUSSION

A panel of mAbs against the purified human placental IGF-IR was previously produced (*14*, *19*). Of those, 1H7, 3B7 and 2C8, which were categorized as belonging to different groups with respect to epitope specificity based on their effects on IGF binding or growth, have become commercially available. Since recombinant antibodies

Table 1. **Summary of binding kinetic analyses of purified mAbs and their respective scFv proteins to IGF-IR.**

Anti-IGF-IR	SPR	ELISA-based
1H7 mAb	3.2×10^{-8}, 1.0×10^{-9} [a]	1.0×10^{-9}
1H7 scFv-Fc	1.0×10^{-8} [a]	1.4×10^{-9}
1H7 scFv	2.3×10^{-8}	2.1×10^{-8}
3B7 mAb	8.6×10^{-9}	ND[b]
3B7R scFv	8.9×10^{-9}	ND[b]

As described in the 'Materials and methods' section two methods by which K_D (M) was obtained were used.
[a]These values are from previously published data (*9*).
[b]Not determined.

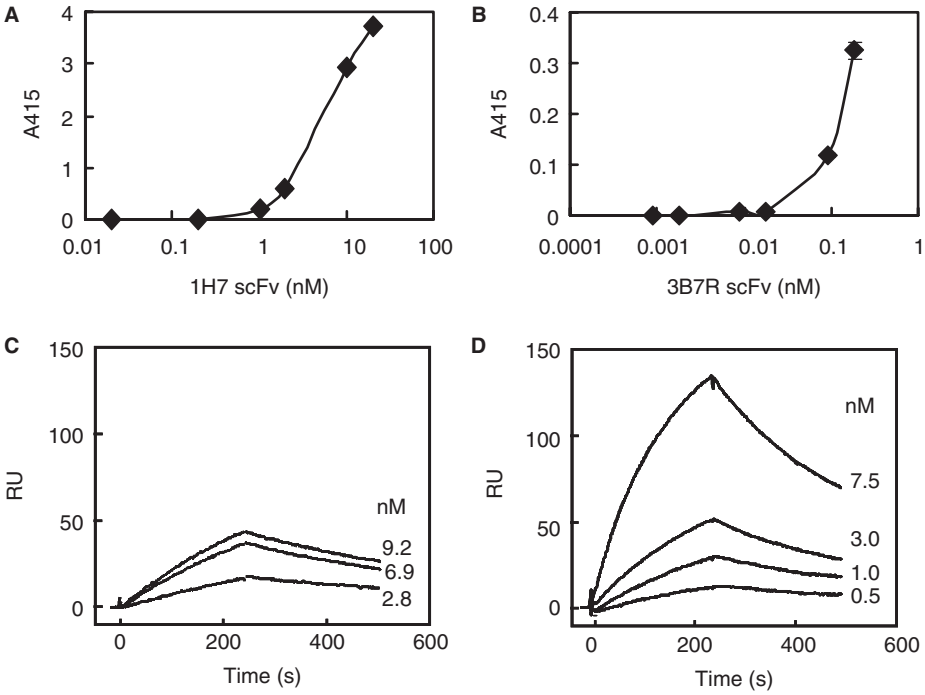

Fig. 8. **Binding of purified 1H7 or 3B7R scFv proteins to IGF-IR.** Purified 1H7 or 3B7R scFv protein at concentrations indicated was analysed for its binding to rhIGF-IR by ELISA (A: 1H7, B: 3B7R) or by SPR (C: 1H7, D: 3B7R) as described in the 'MATERIALS AND METHODS' section. The error bars represent the SD calculated from replicates ($n = 3$) in A and B.

would have been the best strategy for the development of molecular-targeted therapy, a recombinant anti-IGF-I receptor antibody, scFv-Fc, was previously constructed from 1H7 mAb, and its potential as an IGF-IR-targeted cancer therapeutic was demonstrated (*9*, *13*, *15*). While 1H7 mAb inhibits IGF-I binding to IGF-IR, 3B7 mAb enhanced IGF-I binding to the receptor (*14*, *19*), suggesting that the epitope 1H7 mAb binds to must differ from the binding site for 3B7 mAb. This assumption, however, has not been challenged. In this study, phage antibodies were constructed from the variable domains of 1H7 and 3B7 mAb genes derived from respective hybridomas. The competition-binding studies performed using either phage antibodies or soluble scFv proteins with their respective mAbs indeed demonstrated that 1H7 and 3B7 bind to different epitopes on the IGF-IR extracellular domain. Both 1H7 and 3B7 did not bind to the IR extracellular domain. This work also showed that both the VL–VH and VH–VL sequence orders have no apparent effect on their specificity for IGF-IR.

Competition-binding studies were also carried out using other commercially available mAbs 24–57 and 16–13, raised against 3T3 cells expressing high levels of IGF-IR (*20*). Similar to 1H7 and 3B7, mAb 24–57 inhibited IGF binding while 16–13 stimulated IGF binding. The epitopes for mAb 24–57 and 16–13 were earlier shown to be localized to distinct regions of the IGF-IR, residues 440–514 and 62–184 of the α subunit, respectively, using soluble chimeric receptors (*20*, *21*), in which selected regions of the IGF-IR were replaced by corresponding regions of the insulin receptor or *vice versa* (*21*, *28*). Pre-incubation of IGF-IR with mAb 24–57 and 16–13 inhibited binding of 1H7 and 3B7R scFv proteins to the receptor, respectively. This strongly suggested that 1H7 and 3B7 bind to the epitopes that are the same as or near those for mAb 24–57 and 16–13, respectively. As far as 1H7 and 24–57 are concerned. 1H7 apparently binds to a different epitope from that of 24–57 in the α subunit (440–514) domain since their effects on downstream signalling in MCF-7 breast cancer cells differ significantly (manuscript in preparation). Tentative binding domains of 1H7 and 3B7 are shown in the three-dimensional model of IGF-IR as illustrated in Fig. 9 based on published information (*29*). Figure 9 shows the locations of epitopes in the α subunit (62–184) close to N-terminus and the C-terminal domain (440–514), near or to which 3B7 and 1H7, respectively appear to bind.

The present study also revealed affinity constants of purified scFv proteins, which indicated that both 1H7 and 3B7R scFv proteins have high affinity for IGF-IR as a monomer and that 3B7R scFv protein has higher affinity than 1H7 scFv protein. These findings suggest both anti-IGF-IR scFvs are good candidates for development as molecular-targeted therapies. The isolated 1H7 and 3B7R genes can be readily used to design and produce new recombinant molecules by gene manipulation. Such examples include cancer tissue-specific expressions of anti-IGF-IR scFv using specific promoters and production of more effective therapeutic proteins such as anti-IGF-IR scFv conjugated with another antibody or enzyme. The affinity maturation of those scFvs can easily be achieved by phage display technology as well (*30*, *31*).

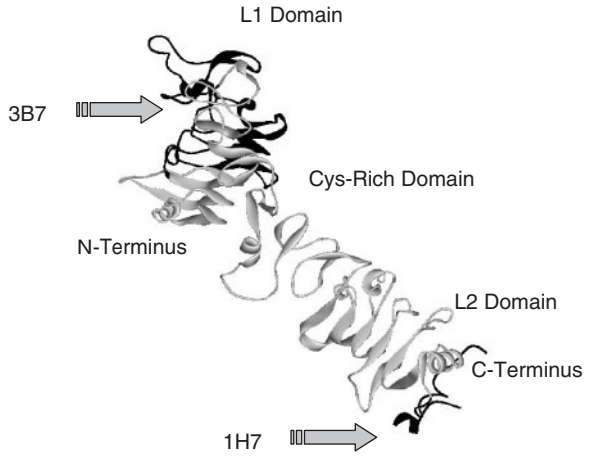

Fig. 9. **Crystal structure of the first three domains of the IGF-IR in relation to epitopes for 1H7 and 3B7 mAbs.** Shown is the crystal structure of the first three domains of the IGF-IR (1–471) consisting of L1, Cys-rich and L2 of the α subunit, the atomic coordinates of which were obtained from Protein Data Bank (RCSB, http://www.rcsb.org/pdb/home/home.do) (*29*). Tentative binding regions for 3B7 and 1H7 mAbs that were identified in this study, 62–184 and 440–514, respectively, are shown in black with arrows. A point of note is that a part of the potential binding region for 1H7 (440–514) is missing in this model which only presents 1–471 residues.

In particular, humanization of the scFvs is essential for development of cancer therapeutics.

In summary, the development of fully human anti-IGF-IR antibodies is now in greater demand for the development and further improvement of cancer therapeutics since the outcome of current clinical trials is forthcoming (*32*) and particularly since increasing evidence suggests that anti-IGF-IR therapy enhances anti-tumour activities of other therapies including anti-EGF receptor therapy, chemotherapy and radiotherapy (*33–36*). This study not only defined the epitope specificity of two of anti-IGF-IR mAbs, but also provided scFv genes as tools for further manipulation of the affinity or development of new IGF-IR-targeted cancer therapeutics.

The authors wish to thank Dr M. Nakata for his kind assistance with the preparation of this manuscript. This work was supported by a grant from the Japan Society for the Promotion of Science and in part by a grant from the JST CREST program.

REFERENCES

1. Ullrich, A., Gray, A., Tam, A.W., Yang-Feng, T., Tsubokawa, M., Collins, C., Henzel, W., LeBon, T., Kathuria, S., Chen, E., Jacobs, S., Francke, U., Ramachandran, J., and Fujita-Yamaguchi, Y. (1986) Insulin-like growth factor I receptor primary structure: comparison with insulin receptor suggests structural determinants that define functional specificity. *EMBO J.* **5**, 2503–2512
2. LeRoith, D., Werner, H., Beitner-Johnson, D., and Roberts, C.T.Jr. (1995) Molecular and cellular aspects of the insulin-like growth factor I receptor. *Endocr. Rev.* **16**, 143–163

3. Baserga, R., Hongo, A., Rubini, M., Prisco, M., and Valentinis, B. (1997) The IGF-I receptor in cell growth, transformation and apoptosis. *Biochim. Biophys. Acta.* **1332**, 105–126
4. Miller, B.S. and Yee, D. (2005) Type I insulin-like growth factor receptor as a therapeutic target in cancer. *Cancer Res.* **65**, 10123–10127
5. Pollak, M.N., Schernhammer, E.S., and Hankinson, S.E. (2004) Insulin-like growth factors and neoplasia. *Nat. Rev. Cancer* **4**, 505–518
6. Larsson, O., Girnita, A., and Girnita, L. (2005) Role of insulin-like growth factor 1 receptor signaling in cancer. *Br. J. Cancer* **92**, 2097–2101
7. Neuenschwander, S., Roberts, C.T.Jr., and Leroith, D. (1995) Growth inhibition of MCF7 breast cancer cells by stable expression of an insulin-like growth factor I receptor antisense ribonucleic acid. *Endocrinology* **136**, 4298–4303
8. Mitsiades, C.S., Mitsiades, N.S., McMullan, C.J., Poulaki, V., Shringarpure, R., Akiyama, M., Hideshima, T., Chauhan, D., Joseph, M., Liberman, T.A., Garcia-Echeverria, C., Pearson, M.A., Hofman, F., Anderson, K.C., and Kung, A.L. (2004) Inhibition of the insulin-like growth factor receptor-1 tyrosine kinase activity as a therapeutic strategy for multiple myeloma, other hematologic malignancies, and solid tumors. *Cancer Cell* **5**, 221–230
9. Li, S.-L., Liang, S.-J., Guo, N., Wu, A.M., and Fujita-Yamaguchi, Y. (2000) Single-chain antibodies against human insulin-like growth factor I receptor: expression, purification, and effect on tumor growth. *Cancer Immunol. Immunother.* **49**, 243–252
10. Hailey, J., Maxwell, E., Koukouras, K., Bishop, W.R., Pachter, J.A., and Wang, Y. (2002) Neutralizing anti-insulin-like growth factor receptor 1 antibodies inhibit receptor function and induce receptor degradation in tumor cells. *Mol. Cancer Ther.* **1**, 1349–1353
11. Maloney, E.K., McLaughlin, J.L., Dagdigian, N.E., Garrett, L.M., Connors, K.M., Zhou, X.M., Blattler, W.A., Chittenden, T., and Singh, R. (2003) An anti-insulin-like growth factor I receptor antibody that is a potent inhibitor of cancer cell proliferation. *Cancer Res.* **63**, 5073–5083
12. Burtrum, D., Zhu, Z., Lu, D., Anderson, D.M., Prewett, M., Pereira, D.S., Bassi, R., Abdullah, R., Hooper, A.T., Koo, H., Jimenez, X., Johnson, D., Apblett, R., Kussie, P., Bohlen, P., Witte, L., Hicklin, D.J., and Ludwig, D.L. (2003) A fully human monoclonal antibody to the insulin-like growth factor I receptor blocks ligand-dependent signaling and inhibits human tumor growth in vivo. *Cancer Res.* **63**, 8912–8921
13. Sachdev, D., Li, S.-L., Hartell, J.S., Fujita-Yamaguchi, Y., Miller, J.S., and Yee, D. (2003) A chimeric humanized single-chain antibody against the type I insulin-like growth factor (IGF) receptor renders breast cancer cells refractory to the mitogenic effects of IGF-I. *Cancer Res.* **63**, 627–635
14. Li, S.-L., Kato, J., Paz, I.B., Kasuya, J., and Fujita-Yamaguchi, Y. (1993) Two new monoclonal antibodies against the α subunit of the human insulin-like growth factor-I receptor. *Biochem. Biophys. Res. Commun.* **196**, 92–98
15. Ye, J.-J., Liang, S.-J., Guo, N., Li, S.-L., Wu, A.M., Giannini, S., Sachdev, D., Yee, D., Brunner, N., Ikle, D., and Fujita-Yamaguchi, Y. (2003) Combined effects of tamoxifen and a chimeric humanized single chain antibody against the type I IGF receptor on breast tumor growth in vivo. *Horm. Metab. Res.* **35**, 836–842
16. Sachdev, D., Singh, R., Fujita-Yamaguchi, Y., and Yee, D. (2006) Down-regulation of insulin receptor by antibodies against the type I insulin-like growth factor receptor: implications for anti-insulin-like growth factor therapy in breast cancer. *Cancer Res.* **66**, 2391–2402
17. Frasca, F., Pandini, G., Scalia, P., Sciacca, L., Mineo, R., Costantino, A., Goldfine, I.D., Belfiore, A., and Vigneri, R. (1999) Insulin receptor isoform A, a newly recognized, high-affinity insulin-like growth factor II receptor in fetal and cancer cells. *Mol. Cell. Biol.* **19**, 3278–3288
18. Sciacca, L., Mineo, R., Pandini, G., Murabito, A., Vigneri, R., and Belfiore, A. (2002) In IGF-I receptor-deficient leiomyosarcoma cells autocrine IGF-II induces cell invasion and protection from apoptosis via the insulin receptor isoform A. *Oncogene* **21**, 8240–8250
19. Xiong, L., Kasuya, J., Li, S.-L., Kato, J., and Fujita-Yamaguchi, Y. (1992) Growth-stimulatory monoclonal antibodies against human insulin-like growth factor I receptor. *Proc. Natl Acad. Sci. USA* **89**, 5356–5360
20. Soos, M.A., Field, C.E., Lammers, R., Ullrich, A., Zhang, B., Roth, R.A., Andersen, A.S., Kjeldsen, T., and Siddle, K. (1992) A panel of monoclonal antibodies for the type I insulin-like growth factor receptor. Epitope mapping, effects on ligand binding, and biological activity. *J. Biol. Chem.* **267**, 12955–12963
21. Schumacher, R., Soos, M.A., Schlessinger, J., Brandenburg, D., Siddle, K., and Ullrich, A. (1993) Signaling-competent receptor chimeras allow mapping of major insulin receptor binding domain determinants. *J. Biol. Chem.* **268**, 1087–1094
22. Engvall, E. and Ruoslahti, E. (1977) Binding of soluble form of fibroblast surface protein, fibronectin, to collagen. *Int. J. Cancer* **20**, 1–5
23. Barbas, C.F. III, Burton, D.R., Scott, J.K., and Silverman, G.J. (2001) *Phage Display: A Laboratory Manual*. pp. 9.53–9.64 Cold Spring Harbor Laboratory Press, New York
24. Cheng, X., Zhang, Y., Kotani, N., Watanabe, T., Lee, S., Wang, X., Kawashima, I., Tai, T., Taniguchi, N., and Honke, K. (2005) Production of a recombinant single-chain variable-fragment (scFv) antibody against sulfoglycolipid. *J. Biochem.* **137**, 415–421
25. Friguet, B., Chaffotte, A.F., Djavadi-Ohaniance, L., and Goldberg, M.E. (1985) Measurements of the true affinity constant in solution of antigen-antibody complexes by enzyme-linked immunosorbent assay. *J. Immunol. Methods* **77**, 305–319
26. Stevens, F.J. (1987) Modification of an ELISA-based procedure for affinity determination: correction necessary for use with bivalent antibody. *Mol. Immunol.* **24**, 1055–1060
27. Dougan, D.A., Malby, R.L., Gruen, L.C., Kortt, A.A., and Hudson, P.J. (1998) Effects of substitutions in the binding surface of an antibody on antigen affinity. *Protein Eng.* **11**, 65–74
28. Kjeldsen, T., Andersen, A.S., Wiberg, F.C., Rasmussen, J.S., Schaffer, L., Balschmidt, P., Moller, K.B., and Moller, N.P. (1991) The ligand specificities of the insulin receptor and the insulin-like growth factor I receptor reside in different regions of a common binding site. *Proc. Natl. Acad. Sci. USA* **88**, 4404–4408
29. Garrett, T.P., McKern, N.M., Lou, M., Frenkel, M.J., Bentley, J.D., Lovrecz, G.O., Elleman, T.C., Cosgrove, L.J., and Ward, C.W. (1998) Crystal structure of the first three domains of the type-1 insulin-like growth factor receptor. *Nature* **394**, 395–399
30. Winter, G., Griffiths, A.D., Hawkins, R.E., and Hoogenboom, H.R. (1994) Making antibodies by phage display technology. *Annu. Rev. Immunol.* **12**, 433–455
31. Marks, J.D., Hoogenboom, H.R., Griffiths, A.D., and Winter, G. (1992) Molecular evolution of proteins on filamentous phage. Mimicking the strategy of the immune system. *J. Biol. Chem.* **267**, 16007–16010
32. Yee, D. (2006) Targeting insulin-like growth factor pathways. *Br. J. Cancer.* **94**, 465–468
33. Wu, J.D., Haugk, K., Coleman, I., Woodke, L., Vessella, R., Nelson, P., Montgomery, R.B., Ludwig, D.L., and Plymate, S.R. (2006) Combined in vivo effect of A12,

a type 1 insulin-like growth factor receptor antibody, and docetaxel against prostate cancer tumors. *Clin. Cancer Res.* **12**, 6153–6160

34. Cosaceanu, D., Carapancea, M., Castro, J., Ekedahl, J., Kanter, L., Lewensohn, R., and Dricu, A. (2005) Modulation of response to radiation of human lung cancer cells following insulin-like growth factor 1 receptor inactivation. *Cancer Lett.* **222**, 173–181
35. Goetsch, L., Gonzalez, A., Leger, O., Beck, A., Pauwels, P.J., Haeuw, J.F., and Corvaia, N. (2005) A recombinant humanized anti-insulin-like growth factor receptor type I antibody (h7C10) enhances the antitumor activity of vinorelbine and anti-epidermal growth factor receptor therapy against human cancer xenografts. *Int. J. Cancer* **113**, 316–328
36. Cohen, B.D., Baker, D.A., Soderstrom, C., Tkalcevic, G., Rossi, A.M., Miller, P.E., Tengowski, M.W., Wang, F., Gualberto, A., Beebe, J.S., and Moyer, J.D. (2005) Combination therapy enhances the inhibition of tumor growth with the fully human anti-type 1 insulin-like growth factor receptor monoclonal antibody CP-751,871. *Clin. Cancer Res.* **11**, 2063–2073